Deformations and Damage Evolution of Austenitic Steel AISI304 with Martensite Phase Transformation

Gang Han[1], HuangYuan[1,2,*]

[1]School of Mechanical Engineering, Beijing Institute of Technology, 100081, China
[2]Department of Mech. Engineering,University of Wuppertal,42097, Germany
* Corresponding author: yuanhuang@bit.edu.cn

Abstract In the present paper martensite transformation in stainless steel 304 and its effects to material damage is discussed. The experiments confirm that martensite phase transformation in SS304 can be described by the Santacreu model and shows dependence on the plastic strain and stress triaxiality. The plasticity model with the martensite transformation is established based on Santacreu model and applied to describe plastic behavior of SS304 with severe plastic deformations. It is shown that the plasticity model predicts strain hardening under both compression and tension uniformly and agrees with experimental results reasonably. Although the fracture strain of SS304 can be characterized by the equivalent plastic strain precisely, fatigue tests display strong influence of the pre-strains to the fatigue life. Whereas the strain-fatigue life curve shows acceleration of fatigue damage in strain-controlled fatigue tests, the stress versus fatigue life curve reveals significantly higher bearing capacity due to pre-strains. This result implies that application of the pre-strain should only be used if the mechanical loading is applied in stress-controlled cases.

Keywords： deformation induced phase transformation, plasticity mode, fatigue damage, fatigue life

1. Introduction

It is known that severe plastic deformations influence material behavior. For instance, surface treatment of critical mechanical parts is an important step in manufacturing. The improvement of fatigue behavior of the mechanical part is realized just due to compressive residual stresses and distortions of the surface material [1-3]. Quantifying effects of surface treatment in fatigue life improvement requires detailed understanding of the mechanical behavior of the material with strong distortion and variation of the residual stresses in the surface layer material. AISI304 is a popular stainless steel and can be found in many industrial branches. On the other side, the stainless steel SS304 is meta stable austenite material, its crystallographic structures can transform to martensite phase under plastic deformations [4-6]. The deformation-induced martensite transformations have been studied for many years, especially in material science communities on kinetics of transformation [7-10].

Due to martensite phase the stainless steel behaviors significantly differently from the austenitic steel, both in plastic deformation and failure [11-15]. Using known models to establish a continuum mechanics model for quantifying effects of surface treatment needs detailed understanding of evolution of microstructure and meso-mechanical behavior of the distorted material [7-10]. Especially, phase transformation under severe compressive deformation is less investigated in the past.

The present work dedicates to identify a plasticity model for SS304 under severe plastic deformations, especially under compressive deformations, and to clarify effects of the pre-strains to material failure under monotonic and cyclic loading. Based on extensive experiments, the plasticity model under consideration of the martensite transformation should be applied to predict fatigue life of the compressive deformed specimens and to quantify effects of the compressive strains to material failure evolution.

2. Plasticity for austenitic steel with martensite phase transformation

2.1 Kinetics of Martensite Transformation

The previous experimental observations confirm that the austenitic steel AISI304 transforms to martensite phase due to plastic deformations. The volume fraction of martensite phase increases with deformations. Olson and Cohen [7] studied the phase transformation and suggested an isotropic phase transformation law that describes the martensite content evolution as a function of plastic strain and temperature. The model was extended by Stringfellow et al [8] by incorporating the dependency of the stress triaxiality. According to the Stringfellow evolution of the martensite content, χ, depends on stress triaxiality η and plastic strain $\bar{\varepsilon}^p$ which reads

$$\dot{\chi} = (1-\chi)\left(A\dot{\bar{\varepsilon}}^p + B\dot{\eta}\right) \tag{1}$$

with the stress triaxiality $\eta = \sigma_m / \sigma_e$ and the equivalent plastic strain $\dot{\bar{\varepsilon}}^p = \sqrt{\frac{2}{3}\dot{\varepsilon}_{ij}^p \dot{\varepsilon}_{ij}^p}$.σ_m and σ_e denote hydrostatic stress and Mises stress, respectively. A and B are model parameters generally depending on the temperature and the stress state. For uniaxial material testing η is constant (η=1/3 for uniaxial tension and -1/3 for uniaxial compression, respectively), so that the martensite content is a monotonic function of the plastic strain and can be expressed as

$$\chi = 1 - \exp\left(-A\bar{\varepsilon}^p\right). \tag{2}$$

The Stringfellow model predicts a monotonic relationship between the stress triaxialityrate without explicit effects of the stress triaxiality. Santacreu et al. [9] suggested an alternative evolution law reads

$$\dot{\chi} = \left(\chi_{\max} - \chi\right) mD\left(D\bar{\varepsilon}^p\right)^{m-1} \dot{\bar{\varepsilon}}^p \tag{3}$$

with

$$D = D_0 + D_1\eta. \tag{4}$$

In the expressions above $\chi_{\max}$ denotes the maximum fraction for martensite transformation, D_1 represent effects of stress triaxiality, m and D_0 denote influences of plastic strain. In the original suggestion of Santacreu et al. [9] the parameter D should further related with the Lode angle, i.e. the third deviatoric stress invariant allowing to build the surface corner in the stress space.

Since $\dot{\bar{\varepsilon}}^p$ is non-negative, the martensite transformation is a monotonic function of time. Therefore, the model only considers austenite-martensite transformation, while the reverse transformation is prohibited. The total form of the Santacreu model reads

$$\chi = \chi_{\max}\left[1 - \exp\left(-\left(D\bar{\varepsilon}^p\right)^m\right)\right] \tag{5}$$

forgiving stress triaxlity.

Both martensite transformation models predict a linear correlation between the plastic strain rate and transformation rate. Stringfellow addressed additionally that the transformation is further influenced by the stress triaxialityrate which is generally rather difficult to be identified in material testing. Furthermore, the martensite transformation may occur for varying stress triaxiality without plastic deformations, which is not confirmed in the stainless steel SS304. A major difference is the explicit expression to the stress triaxiality which allows to apply for FEM computations. In the present work the Santacreu model will be used for considering plasticity of the SS304 under consideration of the martensite transformation.

2.2 Plasticity with phase transformation

The conventional J_2 plasticity is applicable for the present stainless steel without considering

martensite transformation [12]. The potential function is defined as

$$f = \sigma_e - k = 0, \tag{6}$$

where σ_e denotes the effective Mises stress for kinematic hardening, $\sigma_{ij} = \sqrt{\frac{3}{2}\left(s_{ij} - \alpha_{ij}\right)\left(s_{ij} - \alpha_{ij}\right)}$, k is the material resistance against plastic deformation. The backstress is assumed to be

$$\dot{\alpha}_{ij} = \frac{2}{3} c_L \dot{\varepsilon}_{ij}^p - c_{NL} \alpha_{ij} \dot{\bar{\varepsilon}}^p, \tag{7}$$

in the nonlinear kinematic hardening model. According to the associated flow rule the plastic strain rate is proportional to the derivative of the potential function,

$$\dot{\varepsilon}_{ij}^p = \dot{\lambda} \frac{\partial f}{\partial \sigma_{ij}} = \frac{3}{2} \dot{\lambda} \frac{s_{ij} - \alpha_{ij}}{\sigma_e}, \tag{8}$$

where the plastic multiplier $\dot{\lambda} \geq 0$ and the deviatoric stress $s_{ij} = \sigma_{ij} - \sigma_m \delta_{ij}$. The equivalent plastic strain is defined as $\bar{\varepsilon}^p = \int \dot{\bar{\varepsilon}}^p dt = \int \dot{\lambda}\, dt$.

The plasticity model contains both kinematic hardening and isotropic hardening. Whereas the kinematic hardening takes the conventional form [11], the isotropic hardening is affected by martensite transformation and expressed by the deformation resistance,

$$\dot{k} = H_\varepsilon \dot{\bar{\varepsilon}}^p + H_\chi \dot{\chi}, \tag{9}$$

that is, the deformation resistance is linear proportional to plastic strain rate and martensite transformation rate. Both plastic strain hardening modulus, H_ε, and phase transformation hardening modulus, H_χ, are functions of stress and strain states.

Taking the combined hardening model [11] into account, the material resistance under absence of phase transformation can be written as

$$k_\varepsilon = k_0 + H_0 \left[1 - \exp\left(-\beta \bar{\varepsilon}^p\right)\right], \tag{10}$$

with the model parameters k_0 as initial yield stress of the material, H_0 as plastic hardening factor and β hardening exponent. Consequently, the hardening due to plastic deformation can be expressed as

$$H_\varepsilon = \beta H_0 \exp\left(-\beta \bar{\varepsilon}^p\right), \tag{11}$$

The additional phase transformation hardening modulus, H_χ, has to be determined based on experimental observation. Investigation of Beese [10] confirmed a constant modulus H_χ provides sufficient accurate results for steels. Based on the Santacreu model the isotropic hardening can be expressed into

$$\dot{k} = \left[H_\varepsilon + H_\chi \left(\chi_{\max} - \chi\right) m D \left(D \bar{\varepsilon}^p\right)^{m-1} \right] \dot{\bar{\varepsilon}}^p, \tag{12}$$

with H_ε defined in Eq. (11).

Under uniaxial loading condition, the equations can be simplified due to $\sigma_e = \left|\sigma - \alpha\right|$ and $\bar{\varepsilon}^p = \left|\varepsilon^p\right|$ where σ and ε^p are the first principal stress/plastic strain, respectively. The stress-plastic strain curve under monotonic tensile testing can be expressed as

$$\sigma_y = \alpha + k, \tag{13}$$

where the backstress can be evaluated from

$$\alpha = \frac{2 c_L}{3 c_{NL}} \left[1 - \exp\left(-c_{NL} \varepsilon^p\right)\right] \tag{14}$$

and the isotropic hardening stress is expressed as

$$k = k_0 + H_0 \left[1 - \exp\left(-\beta \bar{\varepsilon}^p\right)\right] + \chi_{\max} H_\chi \left[1 - \exp\left(-\left(D \bar{\varepsilon}^p\right)^m\right)\right] \tag{15}$$

with D defined in Eq. (4).In expressions above D and χ_{max} have been identified from the phase transformation curve. The plasticity behavior of the material is described by k_0, H_0, β and H_χ as well as c_L and c_{NL}. In comparing with the conventional combined hardening model [11], one more parameter H_c has to be considered from the tensile tests. Note the formulations above are only valid for monotonic loading.

3. Experiments and Results

3.1 Specimens

In the present work the austenitic stainless steel 304 is investigated, almost versatile and widely used stainless steel and available in a wider range of products. The austenitic structure gives the steel excellent toughness, even down to cryogenic temperatures. The chemical components are summarized in Table 1.

Table 1. Chemical composition of the stainless steel 304

C	Cr	Ni	Mn	Si	P	S	Fe
0.04	17.1	8.1	1.05	0.41	0.035	0.003	bal

Table 2. Mechanical property of the stainless steel 304 after solution treatment

E (GPa)	Ultimate Stress (MPa)	Yield stress (MPa)	Elongation (%)	Hardness (MPa)
200	650	240	100	100

The material used in the present work underwent solution treatment (annealing), heated to 1100°C for 1 hour and cooled down to room temperature in air, to eliminate the residual stresses and initial effects from manufacturing. The mechanical property of the heat treated SS304 is listed in Table 2.

To study effects of deformations to material property, two kinds of specimens have been tested: (1) The plate specimens were fabricated for learning development of Martensite phase in SS304 under tension and compression. The specimen geometry is given in Fig. 1(a). To study development of the martensite phase under compression, the plate specimens can be pressed in the thickness. (2) The tension specimens were taken for tension and fatigue tests, as shown in Fig. 1(b).

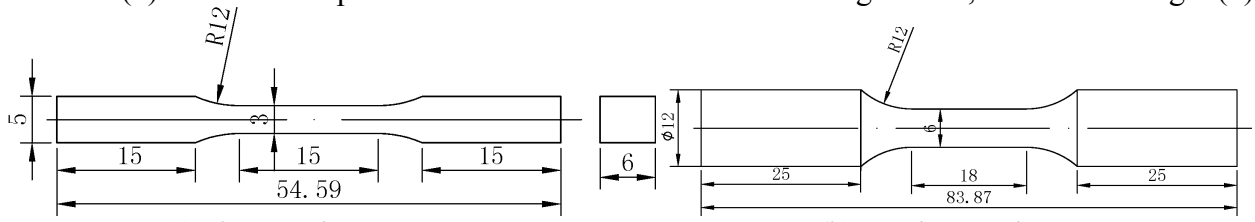

(a) Plate specimen (b) Tension specimen

Figure 1: Specimen geometries tested in the present work. The plate specimens were fabricated for studying martensite phase transformation and the tension bars for fatigue tests.

3.2 Experimental observation of Martensite phase transformation

To quantify evolutions of the martensite phase transformation under compression and it's effects to mechanical property, the plate specimens were pressed in their thickness direction. With various press forces the thickness of the final plate specimens varies between 6mm (0% deformation) and 2.8mm (-53.3% thickness reduction). Mainly ca. -10%, -20%, -30%, -40% and -50% of reduction in specimen thickness were realized. The stress triaxiality under this loading state is η=-1/3.

The tension effects were studies in uniaxial tension specimens after given tensile strains (η=1/3). Five different deformation grades were examined, 20% - 80%. Note the true strain, i.e. the

logarithmic strain, for tension is smaller than the engineering strain, whereas the value of the compressive true strain is generally larger than that of the linear strain. It results in different martensite content for the same deformation grade (engineering strain) in martensite evolution since the martensite evolution law is expressed by the true strain, Eq. (3).

Experimental observations reveal that SS304 is a metastable austenitic steel [16-18]. Figure 2 confirms development of crystallographic pictures of the SS304 after different deformations. The figure demonstrates clearly that the density of martensite needles increases with strains. In pictures dark lines denote martensite phase in the needle form. The pictures reveal that the grain size is ca. 100μm and remains constant even after severe plastic deformations. However, martensite seems proportional increasing with deformations, under both tension and compression. After -45% compression deformations, a large part of austenitic contents in material has been transformed into dark martensite phases. The phase transformation changes and disorders the microstructure of grains, thus arises resistance of the dislocation motions. The material with martensite phase obtains higher strength and less ductility. Experiments do not show significant difference in development of martensite phase under tension from that under compression.

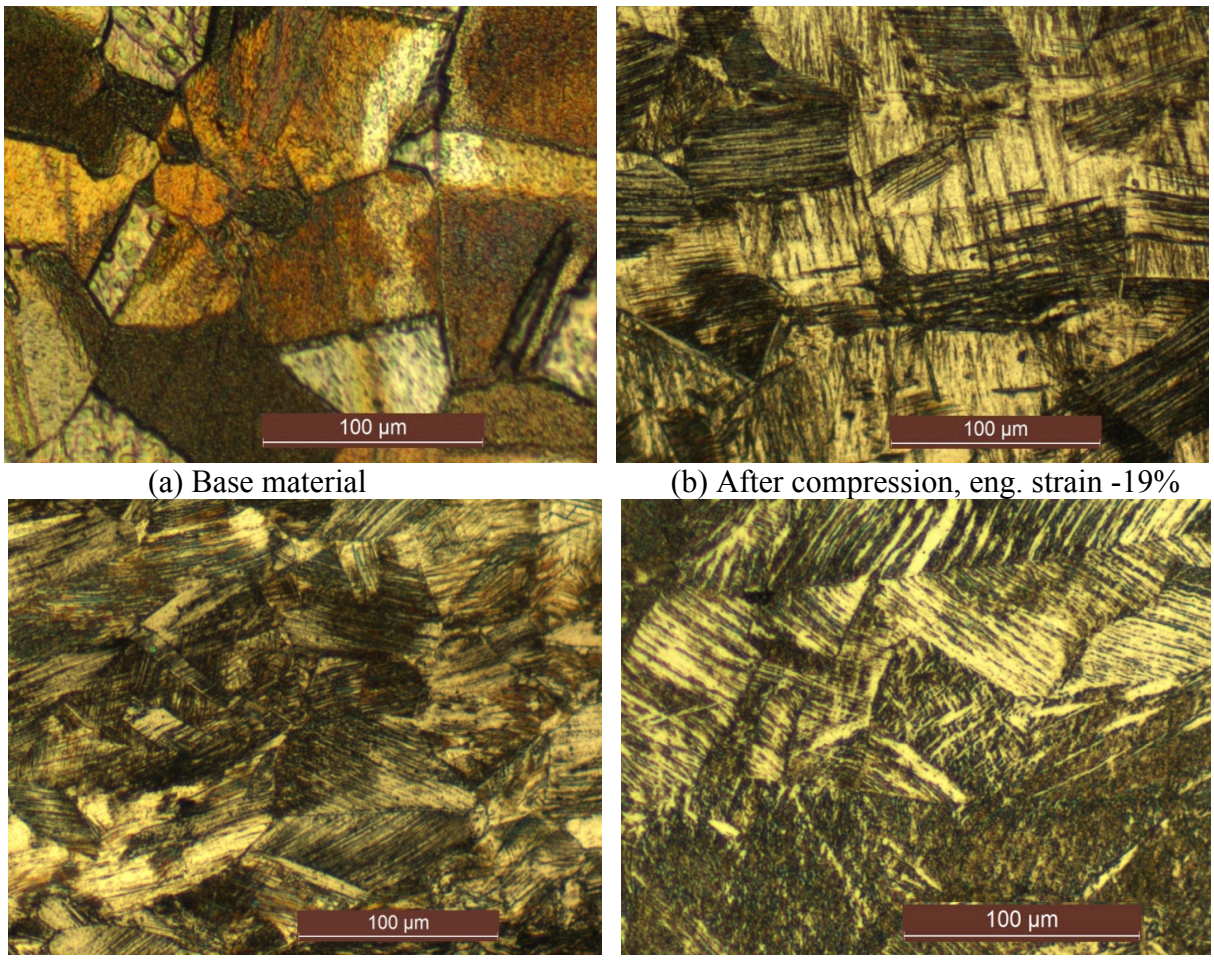

(a) Base material (b) After compression, eng. strain -19%

(c) After compession, eng. strain -45% (d) After tension, eng. strain 40%

Figure 2: Crystallographic pictures of the SS304 after different deformations. The dark phases denote the martensite content.

3.3 Experimental measurement of martensite phase evolution

A ferritescope[19-22] is used to measure the martensite content in the plate specimens. The method measure the martensite content based on changes of the linear relationship between the output

voltage and the magnetic permeability of the sample. If the sample is qualified properly, this method is easy in use and reliable [10, 22].

To study evolution of the martensite phase in SS304, the pre-strained specimens are measured using the ferritescope. The experimental data are shown in Figure 3, in which the martensite content under compressive and tensile uniaxial loading is plotted as a function of the equivalent true plastic strain. Note the true strain, i.e. logarithmic strain, is used here and deviates from the linear engineering strain significantly. The present experimental data reveal that the evolution of the martensite phase in the stainless steel SS304 is determined by the plastic deformation and affected by the stress triaxiality η, but the development seems different from the results in [23].

The solid lines denote prediction from the Santacreu model, Eq. (5), with χ_{max}=1, m=2.55, D_0=1.23 and D_1=0.907. Fig. 3 shows variations of experiments and model predictions. In the present work more general experiments under multi-axial loading condition about evolution of martensite phase are not available. It is an open issue whether or not the stress triaxiality further affects devemopment of the martensite transformation.

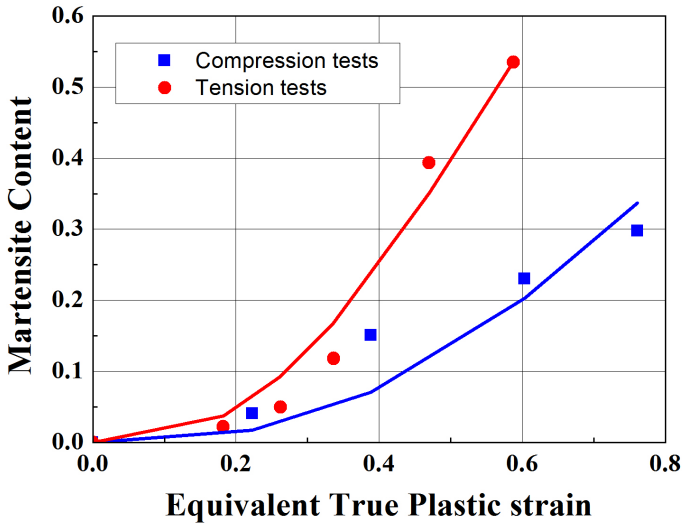

Figure 3: Evolution of the martensite phase in SS304 under both compression and tension. Symbols denote experimental data determined by the ferritescope, whereas the solid lines are predictions from the Santacreu model, Eq. (5).

3.4 Stress-strain relationships

Pre-pressed plate specimens were tested under uniaxial tensile loading condition and the results are summarized in Fig. 4(a). The reduction in the specimen thickness, i.e. pre-strain, varies from 0% (Base material without initial pressing) to 38.6%. The thickness reduction of 38.6% means -48.8% of logarithmic strain. Note that the amplitude of the logarithmic strain under compression is generally larger than the linear strain. In the figure the engineering stress is plotted as a function of the engineering strain which was measured using an extensometer from Epsilon Technology. It is trivial that the stress-strain curves depend on the initial pre-strains. Due to cold work the pressed specimens were broken with smaller strains. Interesting is that the stress increases with the pre-strain significantly.

Under uniaxial loading condition the equivalent plastic strain equals the amplitude of the plastic elongation strain, i.e.

$$\bar{\varepsilon}^p_{eq} = \int \sqrt{\frac{2}{3}\dot{\varepsilon}^p_{ij}\dot{\varepsilon}^p_{ij}}\,dt = \int \dot{\varepsilon}^p\,dt = \sum \Delta\varepsilon^p_i\,, \tag{16}$$

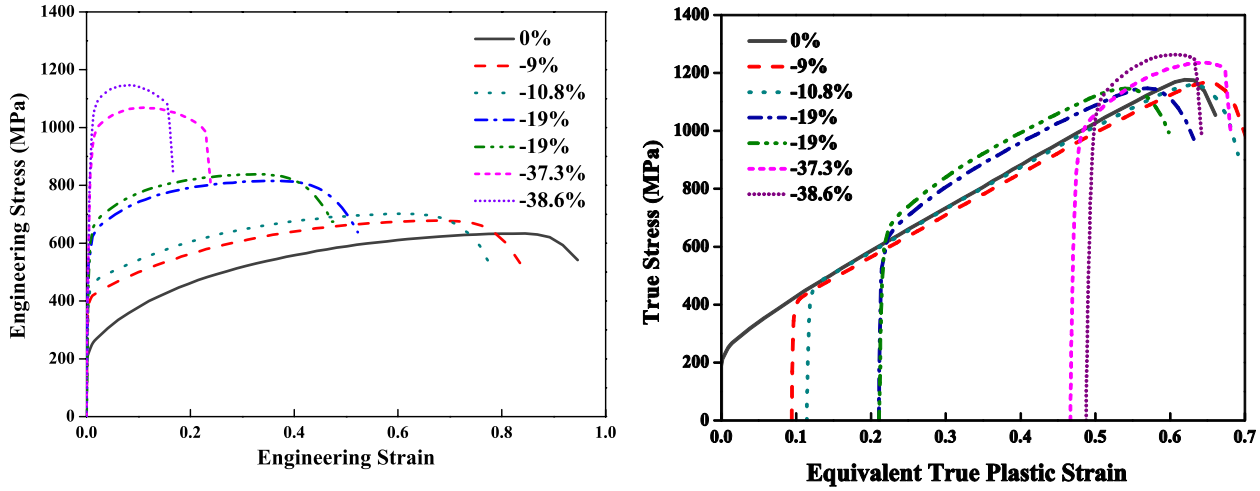

(a) Engineering stress vs. engineering strain curves (b) True stress vs. equivalent true strain curves

Figure 4: Stress-strain curves from tensile tests. The pre-strain was induced by pressing in the thickness. The legends show the reduction of the specimen thickness.

The summation of the plastic strain goes through all loading history. For the pre-strained specimens, the total equivalent plastic strain sums the initial compressive plastic strain and plastic strain under uniaxial tension. The true stress versus total equivalent true plastic strain is shown in Fig. 4(b).

The diagram reveals that the true stress of the tensile specimen is a monotonic function of the plastic strain. Before material damage dominates, the material resistance again deformation grows almost linearly with the plastic strain. The pre-strain induces more resistance than the tension, which implies effects of the anisotropy of the material due to large plastic deformations. If one assumes isotropic material behavior, the anisotropy could be caused by the martensite transformation. The fracture true strains of all specimens exceed 60% and seem less dependent on the pre-strains. The experimental results confirm that the stress-strain curve of SS304 is not so sensitive to the tension or compression, i.e. stress triaxiality.

4. Identification of the plasticity model

Based on the experimental data the plasticity model under consideration of the martensite transformation presented in the previous section can be identified using the least square fitting, Table 3 for the identified parameters. In the table the kinematical hardening in the plastic model is neglected for lacking in corresponding experimental data.

The prediction of the plasticity model under consideration of the martensite transformation is plotted in Fig. 5, together with the experimental data. Reasonable agreement between experiments and model predictions is obtained for all pre-strains, although slight deviations for high pre-strains are observed. Inelastic hardening of specimens can be described by the present plasticity model well.

Table 3.Parameters for constitutive model of the stainless steel 304

Martensite transformation parameters	Plastic isotropic hardening parameters
χ_{max}=1	k_0=220MPa
m=2.55	β=1
D_0=1.23	H_0=2000MPa
D_1=0.907	H_χ=300 MPa

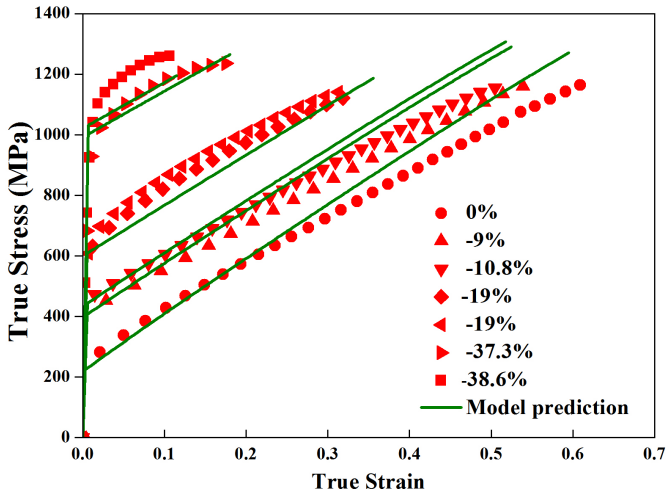

Figure 5: Comparison between experimental data and prediction of the plasticity model under consideration of the martensite transformation.

More results are summarized in Fig. 6, in which true stress at 10% plastic strain and ultimate stress of the SS304 under different pre-strains are plotted. Due to martensite transformation both stress at 10% plastic strain and ultimate stress can be different. The ultimate stress is taken from the maximum stress in the tension tests. The results show, however, that the stress monotonically grows with pre-strain, whereas the ultimate stress of the specimen is independent of initial deformations. Fig. 6(b) shows that the ultimate stress of SS304 is independent of loading history. The prediction of the plasticity model is acceptable.

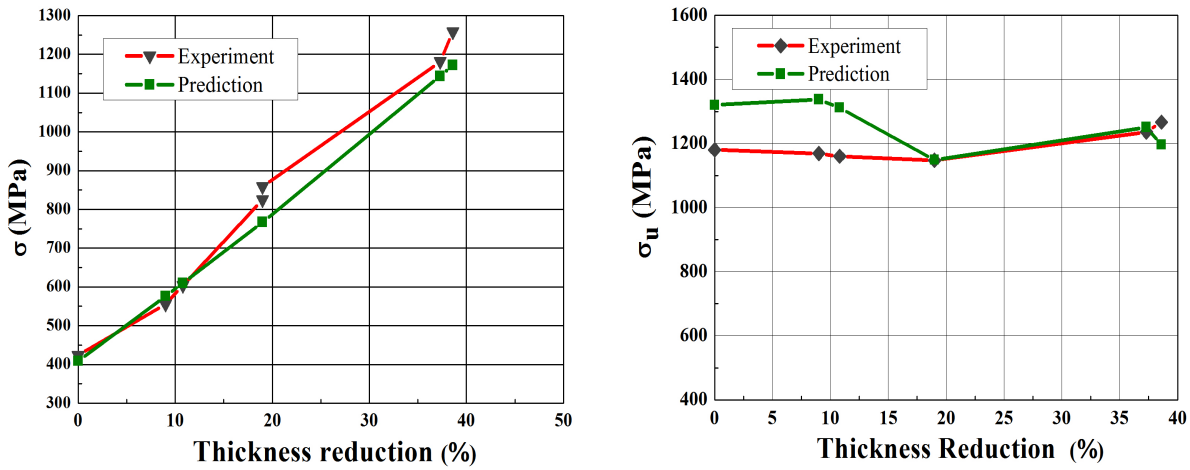

(a) True stress at 10% plastic strain (b) Ultimate stress

Figure 6: Comparison between experimental data and prediction of the plasticity model under consideration of the martensite transformation.

5. Fracture and Fatigue Behavior

Martensite phase transformation affects plastic behavior of the stainless steel SS304. Since H_χ in Eq. (15) is positive, the martensite phase will generally increase the hardening of the material. Due to enbrittlement through martensite phase, however, fracture toughness of SS304 decreases with growth of martensite content. Effects of the martensite phase to material failure have to be

considered carefully.

Figure 7 displays that the fracture strain in the plate specimens decreases with the pre-strain, which seems to be corrected by the total equivalent plastic strain. This result shows the fracture strain for the SS304 is independent of loading history. Martensite transformation seems not to change the fracture strain significantly.

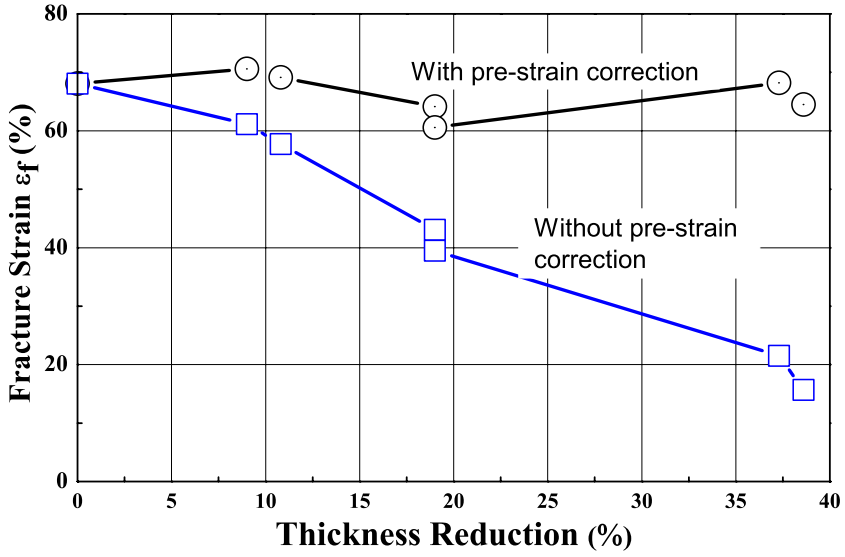

Figure 7: Fracture strains as a function of pre-strains. Fracture strain with pre-strain denotes the total equivalent strain including the initial deformations. The other curves represent fracture strain measured in specimens.

Effects of the pre-strain to fatigue life are not studied systematically. Observations of Miao et al. [14] reveal non-monotonic correlations between LCF life and initial plastic strains. By giving strain amplitudes, stress variations depend on initial treatment of the specimens significantly. In this sense, stress-controlled tests provide totally different results than the strain-controlled tests.

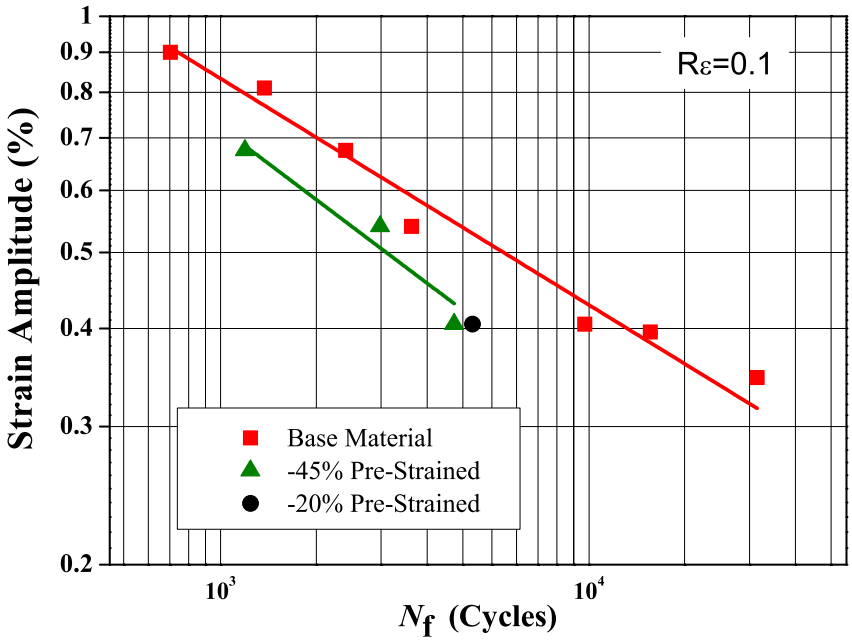

Figure 8: Strain-fatigue life curves for both base material and pressed material from strain-controlled fatigue tests.

In the present work several pre-strained tensile specimens were tested under given strain amplitude with the loading ratio 0.1. The results are shown in Fig. 8. From the diagram one sees that the pre-strain reduces LCF fatigue life of the specimen. In the figure the fatigue life is expressed in the form of Basquin model

$$\varepsilon_a = A\left(N_f\right)^m, \tag{17}$$

with A and m as material specific parameters. For the base material it was identified A=7.034 and m=-0.3083. For the pre-strained specimen A=8.322 and m=-0.35. This result implies that the pre-strained specimen loses almost 50% LCF life of the original untreated specimen. The grade of pre-strain seems to affect fatigue damage secondarily. One major for the life reduction is caused by the significant difference in applied stress amplitude. Due to huge strain hardening induced by plastic deformations and martensite phase transformation in pre-straining treatment, the pre-strained specimens are significantly high strengthed than the base material. It follows that the pre-strained specimens were under much higher stresses than the base material specimens, by giving strain amplitudes, as shown in Fig. 9. The stress amplitude in Fig. 9 is the final stabilized stress amplitude in strain-controlled fatigue tests. From the figure one learns that the pre-strained specimens are much stronger than the base material specimens, that is, by giving fatigue life, the pre-strained specimens can bear much higher mechanical loads.

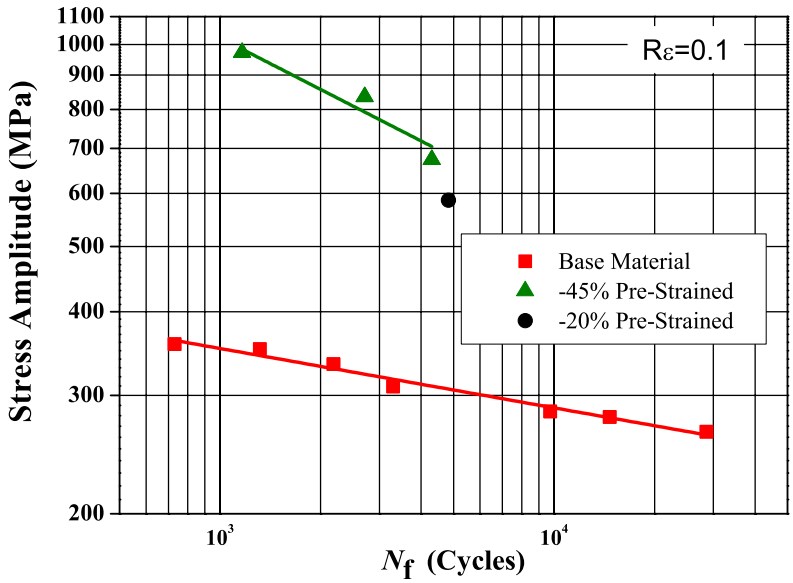

Figure 9: The stabilized stress amplitude as a function of fatigue life from strain-controlled fatigue tests.

6. Conclusions

In the present paper a systematical work on martensite transformation in stainless steel 304 and its effects to material damage is presented. The first experiments confirm that matensite phase transformation in SS304 can be described by the Santacreu model and shows significant dependence on stress triaxiality.

The plasticity model with the martensite transformation is established based on after Santacreu model and can be applied to describe plastic behavior of SS304 with severe plastic deformations. The plasticity model predicts strain hardening under both compression and tension uniformly. Computational predictions agree with experimental results reasonably.

Although the fracture strain of SS304 can be characterized by the equivalent plastic strain precisely, fatigue tests display strong influence of the pre-strains to the fatigue life. Whereas the strain-fatigue life curve shows acceleration of fatigue damage in strain-controlled fatigue tests, the stress versus fatigue life curve reveals significantly higher bearing capacity due to pre-strains. This result implies

that application of the pre-strain should only be used if the mechanical loading is applied in stress-controlled cases.

References

[1] Schulze V. Modern Mechanical Surface Treatment – States, Stability, Effects. Wiley-VCH Verlag GmbH &Co. KGaA. 2006.
[2] Altenberger I, Nalla RK, Noster U, Liu G, Scholtes B. Residual tress stability and near-surface microstructures in high temperature fatigued mechanically surface treated Ti-6Al-4V. Materialwissenschaft und Werkstofftechnik, 34 (2009) 29 – 541.
[3] Liu J, Yuan H. Prediction of residual stress relaxations in shot-peened specimens and its application for the rotor disc assessment. Materials Science and Engineering, A 527 (2010) 6690–6698.
[4] V. Mertinger, E. Nagy, F. Tranta, J. Sólyom, Strain-induced martensitic transformation in textured austenitic stainless steels. Materials Science and Engineering: A, 481–482 (2008) 718-722.
[5] S.S.M. Tavares, D. Gunderov, V. Stolyarov, J.M. Neto, Phase transformation induced by severe plastic deformation in the AISI 304L stainless steel. Materials Science and Engineering: A, 358 (2003) 32-36.
[6] S.K. Ghosh, P. Mallick, P.P. Chattopadhyay, Effect of cold deformation on phase evolution and mechanical properties in an austenitic stainless steel for structural and safety applications. Journal of Iron and Steel Research, International, 19 (2012) 63-68.
[7] G.B. Olson, M. Cohen, Kinetics of strain-induced martensitic nucleation. Metallurgical Transactions A, 6 (1975) 791-795.
[8] R.G. Stringfellow, D.M. Parks, G.B. Olson, A constitutive model for transformation plasticity accompanying strain-induced martensitic transformations in metastable austenitic steels. ActaMetallurgica et Materialia, 40 (1992) 1703-1716.
[9] PO Santacreu, JC Glez, G Chinouilh, T Frölich. Behaviour model of austenitic stainless steels for automotive structural parts. Steel Research International, 77(2006) 686-691.
[10] A.M. Beese, D. Mohr, Effect of stress triaxiality and Lode angle on the kinetics of strain-induced austenite-to-martensite transformation. Acta Materialia, 59 (2011) 2589-2600.
[11] J.L. Chaboche, A review of some plasticity and viscoplasticity constitutive theories. International Journal of Plasticity, 24 (2008) 1642-1693.
[12] J. Lublin. Plasticity theory. Pearson Educational Inc., 2006.
[13] Socie DI, Marquis GB. Multiaxial Fatigue, SAE International, Arrendale, 2000.
[14] C.J. Miao et al. Investigation of low-cycle fatigue behavior of austenitic stainless steel for cold-stretched pressure vessels. Journal of Zhejiang University- Science A (Applied Physics and Engineering), 14(2013): 31-37.
[15] Z. Mei, J.W. Morris, Influence of deformation-induced martensite on fatigue crack propagation in 304-type steels, Metallurgical Transactions A, 21 (1990) 3137-3152.
[16] A. Das, S. Sivaprasad, M. Ghosh, P.C. Chakraborti, S. Tarafder, Morphologies and characteristics of deformation induced martensite during tensile deformation of 304 LN stainless steel. Materials Science and Engineering: A, 486 (2008) 283-286.
[17] K. Mumtaz, S. Takahashi, J. Echigoya, Y. Kamada, L. F. Zhang, H. Kikuchi, K. Ara, M. Sato, Magnetic measurements of martensitic transformation in austenitic stainless steel after room temperature rolling. Journal of Materials Science, 39 (2004) 85– 97.
[18] W.S. Lee, C.F. Lin, The morphologies and characteristics of impact-induced martensite in 304L stainless steel, ScriptaMaterialia, 43 (2000) 777-782.
[19] G. Hu, C.C. Xu, J.G.Yuan, Deformation induced martensite transformation and its magnetic memory effect of austenitic 304 stainless steel. Nondestructive Testing, 30(2008)216-219.
[20] Y.X. Ren, The comparison test of α-phases of austenite and ferrite austenite double phases of stainless steel,Physical Testing and Chemical Analysis Part A:Physical Testing, 41(2005) 184-185.
[21] C.C. Xu, X.S.Zhang, G.Hu, Microstructure change of AISI304 stainless steel in the course of cold working. Journal of Beijing University of Chemical Technology (Natural Science Edition), 29(2002) 27-31.
[22] J. Talonen, P. Aspegren, H. Hanninen, Comparison of different methods for measuring strain induced alpha' -martensite content in austenitic steels, Materials Science and Technology, 20 (2004) 1506-1512.
[23] C.C Young, Transformation toughening of phosphocarbide-strengthened austenitic steels. Doctoral thesis, Massachusetts Institute of Technology, Cambridge, MA, USA, 1988.